Mapana – Journal of Sciences
2025, Vol. 24, No. 2, *61-75*
ISSN 0975-3303 | https://doi.org/10.12723/mjs.73.4

Insight into Indole Derivatives by Experimental and Theoretical Methods

Vijayalaxmi Mallayya*, Srinath*, Omnath Patil*, Nagesh G. Y.†, S. M. Hanagodimath*

Abstract

Solvent effect on fluorescence and absorption spectra of fluorescent Indole derivative viz, 5-chloro-3-phenyl-1H-indole-2-carbohydrazide (CPIC), is studied in different solvents at room temperature. The shifts in the position, intensities and shapes of the absorption and fluorescence bands are observed. The ground and excited state dipole moment of the fluorescent molecule are calculated from the Solvatochromic shift method. The excited-state dipole moments were estimated from Lippert, Bakhshiev and Kawski–Chamma–Viallet equations by using the variation of the Stokes' shift with the solvent dielectric constant and refractive index. The Reichardt's microscopic solvent polarity parameter is used to calculate the change in dipole moment. It is found that the excited-state dipole moments were higher than those of the ground-state dipole moment. The large value of dipole moment in the excited state is due to the increased polar nature. The HOMO-LUMO energy gap and MEP map are estimated theoretically by using B3LYP/6-31+G (d, p) basis set of the Gaussian 16 program.

Keywords: Electric Dipole moment, HOMO-LUMO, Molecular Electrostatic Potential.

1. Introduction

Indole is also known as benzopyrrole, which contains the benzenoid nucleus and has 10 π- electrons (two from ion pair on nitrogen and double bonds provide eight electrons), which makes it aromatic in nature. Like the benzene ring, electrophilic substitution occurs readily on indole due to excessive delocalization of the π-electrons. Indole is an important heterocyclic system that provides the indole skeleton, occurs in a variety of natural

* Department of Physics, Gulbarga University, Kalaburagi 585106. India; mallayyalaxmi49@gmail.com
† Department of Chemistry, Guru Nanak First Grade College, Bidar, Karnataka, India

products, predominantly in alkaloids, and is seldom used for the plan of many synthetic compounds with powerful pharmacological activities [1]. In addition, indole is a privileged scaffold in drug discovery programs and its associated biological activities are very much cited in the literature. Indole based compounds act as efficient dye sensitized solar cells [2] and has diverse application in the field of biological sciences [3-5], as chemical sensors, fluorescent probes, laser dyes and non-linear optical devices. Indole composites are used as, antimicrobial, anti-cancer, anti -inflammatory, anti-anxiety, anti-depressant, rodenticides and fluorescent indicators [6-11]. DFT is used to investigate the characteristics of a substance and explain some experimental occurrences. So theoretical research may be used to measure experimental results. We also performed DFT in this regard. There has been no research done on this sort of chemical, as per the literature review. This aroused our interest in the indole derivative [CPIC], which is the subject of our current study.

2. Materials and methods

The indole derivative, namely 5-chloro-3-phenyl-1H-indol-2-carbohydrazide [CPIC], was synthesised by using the reported method [7]. The molecular structure of the fluorescent molecule is given in **Fig.1a**. The solvents used for the present work, DMSO (Dimethyl Sulfoxide), DMF (Dimethylformamide), Acetonitrile, Acetone, THF (Tetrahydrofuran), Ethyl acetate, DEE (Diethyl ether), Benzene, 1, 4- Dioxane and Toluene were procured from S. D. Fine Chemicals Ltd. India and all the solvents were of HPLC spectroscopic grade and were used without any further purification. The required solutions were prepared at a fixed solute concentration ($1x10^{-5}$ M/L). In order to minimise the effect of self-absorption, the concentration of solute was kept sufficiently low. Absorption spectra were recorded on a PG Inst. Ltd., model T-90+, UV–Visible absorption spectrophotometer, and fluorescence spectra on FP-8300 Fluorescence Spectrometer.

3. Theoretical background

3.1. Estimation of Ground (μ_g) and Excited State (μ_e) Dipole Moments

The influence of solvent polarity on the indole derivative was studied by using Solvatochromic shift method in solute-solvent mixtures. This method is based on the Onsager's reaction field theory, which gives a description of non-specific electrostatic interaction. The independent equations used to estimate ground and excited state dipole moments of the indole derivatives in various solvent of varying dielectric constant (ε) and refractive index (n) are [12-16].

Lippert-Mataga Equation

$$\bar{\nu}_a - \bar{\nu}_f = m_1 F_1(\varepsilon, n) + Constant \quad (1)$$

Bakhshiev"s equation

$$\bar{\nu}_a - \bar{\nu}_f = m_2 F_2(\varepsilon, n) + Constant \quad (2)$$

Kawaski Chamma Vialette's equation

$$\frac{\bar{\nu}_a + \bar{\nu}_f}{2} = -m_3 F_3(\varepsilon, n) + Constant, \quad (3)$$

where *a* and *f* represent the absorption and fluorescence maxima wavenumbers in cm^{-1} respectively, and solvent polarity functions F_1, F_2, and F_3 are provided below.

$$F_1(\varepsilon, n) = \left[\frac{\varepsilon - 1}{2\varepsilon + 1} - \frac{n^2 - 1}{2n^2 + 1}\right] \quad (4)$$

$$F_2(\varepsilon, n) = \left[\frac{\varepsilon - 1}{\varepsilon + 2} - \frac{n^2 - 1}{n^2 + 2}\right] \frac{(2n^2 + 1)}{(n^2 + 2)} \quad (5)$$

$$F_3(\varepsilon, n) = \frac{2n^2 + 1}{2(n^2 + 2)} \left[\frac{\varepsilon - 1}{\varepsilon + 2} - \frac{n^2 - 1}{n^2 + 2}\right] + \frac{3(n^4 - 1)}{2(n^2 + 2)^2} \quad (6)$$

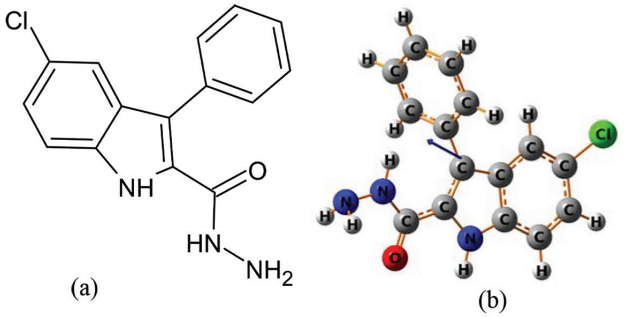

Fig.1 (a) Molecular structure and (b) Optimized geometry with a vector dipole moment of CPIC

The meanings of ε and *n* are as usual. The plots of $\bar{\nu}_a - \bar{\nu}_f$ v/s $F_1(\varepsilon, n)$, $F_2(\varepsilon, n)$ and $\frac{\bar{\nu}_a + \bar{\nu}_f}{2}$ versus $F_3(\varepsilon, n)$ have been plotted respectively and the slopes m_1, m_2 and m_3 are obtained respectively, as shown below.

$$m_1 = \frac{2(\mu_e - \mu_g)^2}{hca_0^3} \quad (7)$$

$$m_2 = \frac{2(\mu_e - \mu_g)^2}{hca_0^3} \quad (8)$$

$$m_3 = \frac{2(\mu_e^2 - \mu_g^2)}{hca_0^3} \quad (9)$$

The dipole moments μ_e and μ_g indicate the excited-state and ground-state dipole moments of an indole molecule. The letters *a* denote the Onsager's cavity radius of the solute molecule, where *h* is Planck's constant and *c* is the velocity of light. Edward [17] uses the microscopic increment method to estimate *a* value. The following Eqs (10) and (11) are obtained on the basis of Eqs (8) and (9)

$$\mu_g = \frac{m_3 - m_2}{2}\left[\frac{hca_0^3}{2m_2}\right]^{\frac{1}{2}} \quad (10)$$

$$\mu_e = \frac{m_3 + m_2}{2}\left[\frac{hca_0^3}{2m_2}\right]^{\frac{1}{2}} \quad (11)$$

3.2. Molecular-Microscopic Solvent Polarity Parameter $\left(E_T^N\right)$

H-bonding or polarisation dependency on spectral characteristics may be studied utilizing E_T^N. Reichardt [18] proposed that spectral shift and E_T^N are related. Reichardt and Ravi et al. proposed the association between the Stokes shift and E_T^N in their various theories. Accordingly, eq^n (12) is obtained.

$$\bar{\nu}_a - \bar{\nu}_f = 11307.6\left[\frac{\Delta\mu^2 a_B^3}{\Delta\mu_B^2 a_0^3}\right] E_T^N + Constant, \quad (12)$$

where $\Delta\mu = 9$ D and $a_B = 6.2$ Å are the change in dipole moment on excitation. The change in dipole moment can be evaluated from the slope of the stokes shift versus E_T^N plot and is given by Eq (13)[18].

$$\Delta\mu = \mu_e - \mu_g = \sqrt{\frac{m \times 81}{\left[\frac{6.2}{a}\right]^3 x\ 11307.6}} \quad (13)$$

where *m* is the slope of the linear plot of E_T^N vs Stokes shift.

Kamlet and co-workers, proposed the multilinear regression (MLR) method based on linear solvation energy relationship to study the solute-solvent interactions of the probe as a function of solvent polarity. MLR- method

shows relationship between stokes shift and absorption transition energy with an index of the ability of solvents polarity. This method is a measure of the ability of solvents to stabilize a charge/dipole through indices of the solvent's hydrogen bond donor (HBD) strength (∝) [42], hydrogen bond acceptor (HBA) strength (β) and non-specific dielectric interactions (π)*, according to eq (11).

$$Y=y_0+a\alpha+b\beta+c\pi^* \quad (14)$$

where a, b, and c represent the measurements of solvent HBD ability, HBA ability, and non-specific dielectric interactions, respectively. The spectroscopic property of interest is represented by y, and y_o represent the intercept value corresponding to the gas phase's spectroscopic property.

$$Y=y_0+dSA+eSB+fSP, \quad (15)$$

where SA, SB, and SP are scales that describe acidity, basicity and polarizability/dipolarity of the solvents, respectively. d, e and f are regression co- efficients [19-20].

3.3. Quantum Chemical Mechanics

By employing the aforementioned chemical approach of quantum mechanics, we calculated the theoretical dipole moment of the derivative in its lowest energy state, denoted as μ_g. This allowed us to optimize the ground state geometry of CPIC by employing the B3LYP hybrid DFT method with a basis set of 6 –31 + G (d, p). The Gaussian 16W program was used to carry out the calculations [21-25].

4. Results and Discussion

4.1. Solvent Effect on Absorption and Fluorescence Emission Spectra

The CPIC normalized absorption and emission spectra in various solvents are displayed in **Fig. 2 (a) and Fig. 2 (b)** respectively. Molecular structure and optimized geometry with a dipole moment vector of CPIC in **Fig.1(b)** correspond to wavelengths varying from 270 to 330 nm and 410 nm to 420 nm in different solvents respectively [26]. When comparing the emission and absorption spectra, there is a greater shift in the former. The dielectric constant of the solvents used is the cause of the shift in the CPIC emission and absorption maxima. To collect the emission spectra, the sample was excited at its maximum absorption [27]. The ICT transition has been found to be the longest wavelength absorption band, and the excitation maxima are located in this band. The stoke shift, arithmetic mean, and maxima of the derivative's emission and absorption in various solvents are shown in **Table 1**. The absorption spectra of CPIC exhibit a spectral band shift

upon switching the solvent from polar aprotic acetonitrile and non-polar 1,4-Dioxane. The values are 278 nm, and 318 nm, respectively, and the spectral band shift in emission spectra of 389 nm, and 403 nm respectively, to a polar aprotic acetonitrile and a non-polar 1,4-dioxane. This means that variations in solvent polarity and hydrogen bonding properties have an impact on this derivative's ground-state energy distribution. The comparison of the derivative's emission maxima in 1,4-dioxane, and acetonitrile indicates that solvents' hydrogen bonding properties have a greater impact on the CPIC derivative's emission properties. 1,4-dioxane, acetonitrile, exhibit Stokes shifts of 6633 cm^{-1}, and 10265 cm^{-1}, respectively.

Table 1: Absorption maxima, emission maxima, corresponding wave-numbers, Stokes shift, arithmetic stokes shifts and energy gap for CPIC in solvents.

Solvents	λ_a	λ_f	$\bar{\nu}_a$	$\bar{\nu}_f$	$\bar{\nu}_a - \bar{\nu}_f$	$\left(\frac{\bar{\nu}_a + \bar{\nu}_f}{2}\right)$
DMSO	310	408	32258	24509	7749	28383
DMF	299	397	33444	25188	8256	29316
Acetonitrile	278	389	35971	25706	1026	30838
Ethyl acetate	287	393	34843	25445	9398	30144
Hexane	296	381	33783	26246	7537	30014
Benzene	317	394	31545	25380	6165	28462
1,4-Dioxane	318	403	31446	24813	6633	28129
Toluene	317	391	31545	25575	5970	28560
Cyclohexane	260	393	38461	25252	1320	31856

This implies that the Stokes shift value rises with solvent polarity. Furthermore, the derivative's fluorescence band maxima redshift as solvent polarity rises. The redshift that increases with solvent polarity suggests that the $\pi \rightarrow \pi^*$ transition may be at play. In the excited state, more intermolecular interaction with almost doubles causes the fluorescence band to shift towards a larger wavelength. This implies that ICT contributes to a more relaxed mood [28–30]. Together with the microscopic solvent polarity function, the dielectric constants, refractive indices, and corresponding polarity functions were computed and are displayed in **Table 2**. **Fig 3** displays how the polarity functions and arithmetic Stokes shifts changed, as well as how the polarity of microscopic solvents changed with Stokes shifts.

Table 2: The dielectric constant, refractive index and polarity functions of respective solvents.

Solvent	ε	**n**	$F_1(\varepsilon, n)$	$F_2(\varepsilon, n)$	$F_3(\varepsilon, n)$	E_T^N
DMSO	46.7	1.477	0.264	0.841	0.743	0.444
DMF	36.7	1.431	0.274	0.836	0.710	0.386

Solvent	ε	n	$F_1(\varepsilon,n)$	$F_2(\varepsilon,n)$	$F_3(\varepsilon,n)$	E_T^N
Acetonitrile	37.5	1.344	0.305	0.863	0.666	0.460
THF	7.58	1.407	0.210	0.549	0.551	0.207
EA	6.02	1.422	0.182	0.466	0.520	0.228
Hexane	1.89	1.375	-0.001	-0.002	0.253	0.253
Benzene	2.28	1.501	0.003	0.006	0.334	0.111
1 4-Dioxane	2.22	1.422	0.022	0.044	0.325	0.164
Toluene	2.38	1.429	0.035	0.072	0.288	0.099
Cyclohexane	2.02	1.426	-0.002	-0.003	0.272	0.006

4.2. Estimation of ground and excited state dipole moments

The dipole moment of the ground state was estimated using two methods: The basis set for the B3LYP hybrid DFT approach and the solvatochromic shift method was 6–31 + G (d, p). Using the previously described quantum chemical method, we theoretically optimize the ground state shape of the CPIC derivative. The optimized geometry and molecular structure with the CPIC derivative's dipole moment vector are shown in **Fig. 1** [31–33].

The solvatochromic shift method is used in the experiment to measure the ground-state dipole moment. The observations show a small discrepancy between the observed and predicted ground-state dipole moment values. In contrast to theoretical and experimental results determined using ab initio DFT calculations, the ground state dipole moment has changed as a result of the derivative's radius being taken into consideration while calculating the dipole moment of the ground state. However, ab initio calculations only yield values for derivatives in a gas phase, whereas experimental methods take solvent effects and environmental factors into account [34–36]. This could be the cause of the discrepancy between the experimental and theoretical values of the derivative's dipole moment.

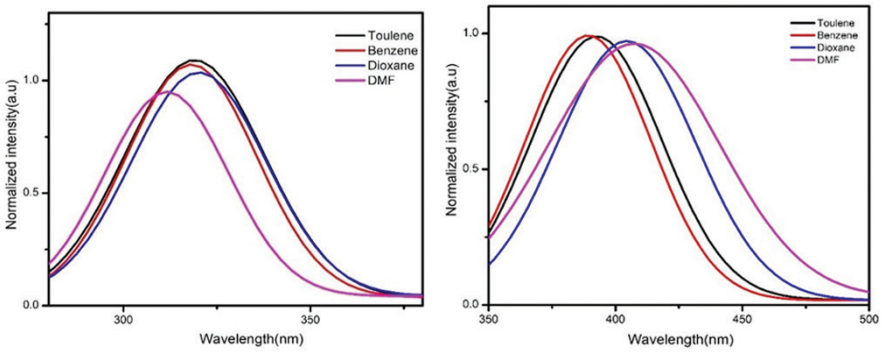

Fig 2: (a) Absorption spectra and (b) Fluorescence spectra of CPIC in selected solvents

Table 3: Values of radius, ground state, excited state, and change in dipole moment of CPIC in Debye

Compound	Radius (r) in Å	μ_g^a	μ_e^b	μ_e^c	μ_e^d	μ_e^e	$\Delta\mu^f$	$\Delta\mu^g$	$\frac{\mu_e}{\mu_g}$
CPIC	3.58	0.64	5.53	10.4	5.53	5.53	4.83	4.93	8.64

1 Debye (D) = 3.33564X10^{-30}cm = 10^{-18} esu cm.

[a] The ground states dipole moments calculated using Eq. (10)

[b].The excitated state dipole moment calculated by Eq. (11)

[c] The experimental excited state dipole moments calculated from Lippert's equation.

[d]The experimental excited state dipole moments calculated from Bakhshiev's equation.

[e]The experimental excited state dipole moments calculated from Chamma-Viallet's equation.

[f] The change in dipole moments from Eq. (10) and (11).

[g]The change in dipole moments calculated from Eq. (12)

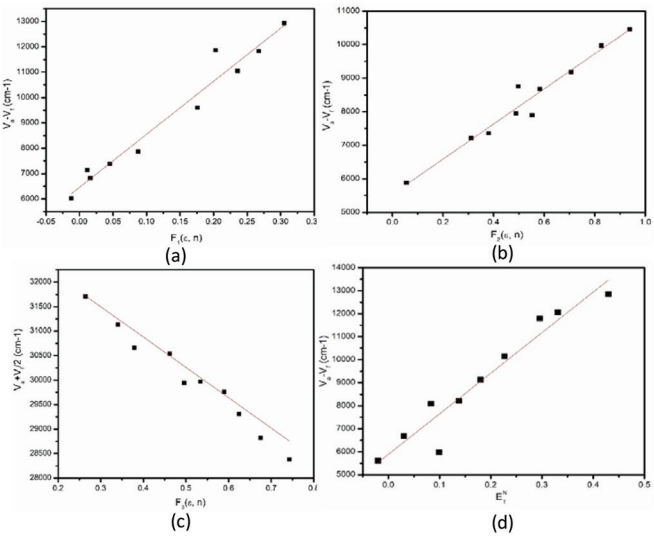

Fig 3: Variations of Stoke's shifts with polarity functions, (a) Lippert, (b) Bakhshiev's, (c) Kawski-Chamma-Viallet's, and (d) Microscopic solvent polarity (E_T^N) functions for CPIC

4.3. Analysis of quantum chemical calculation

4.3.1. Molecular orbital analysis

As shown in Fig. 3, molecular orbitals may be utilised to depict the chemical reactivity, active sites, and kinetic stability of different molecules. The

highest and lowest unoccupied molecular orbitals are called the HOMO and LUMO, respectively. The molecule's LUMO indicates its ability to receive electrons, and it LUMO indicates its ability to donate them. DFT/B3LYP was used to predict the molecular orbital boundary based on 6-31+G (d, p). One of the most important analytical parameters for determining a compound's transference characteristics is the energy changes between these chemical orbitals [36–37]. From Fig 4 and Fig 5, it is evident that the energy gap value by experiment is much larger than the theoretically estimated value of the molecule. It is due to the solvent effect on the molecule, but there was no such effect on the molecule by computational calculations because computational calculation is performed in the gas phase.

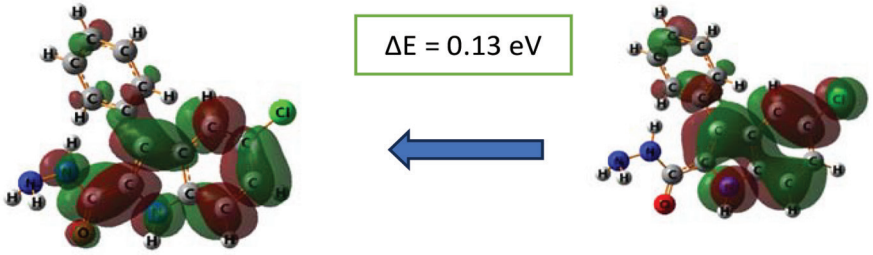

Fig. 4: HOMO - LUMO Energy gap

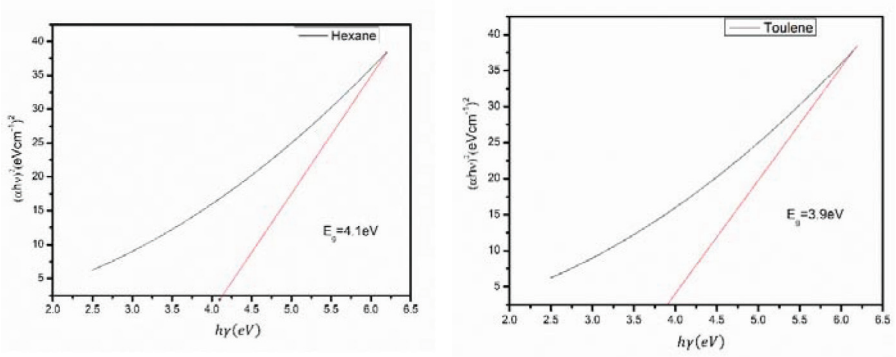

Fig. 5: Tauc pots for CPIC in (a) Hexane and (b) Toluene

4.3.2. Molecular electrostatic potential

In three-dimensional systems, the charge distributions of molecules are depicted by electrostatic potential maps. A nucleophilic attack has a maximum electrostatic potential of blue, whereas an electrophilic attack has a minimum electrostatic potential of red [19–20]. Compound MPIC's MEP is produced and mapped using geometry optimization. The MEP diagram's colour code for CPIC ranges from -5220 a.u. (dark red) to 5220 a.u. (dark blue). The 3D mapped MEP is displayed in the **Fig 6** [38–40].

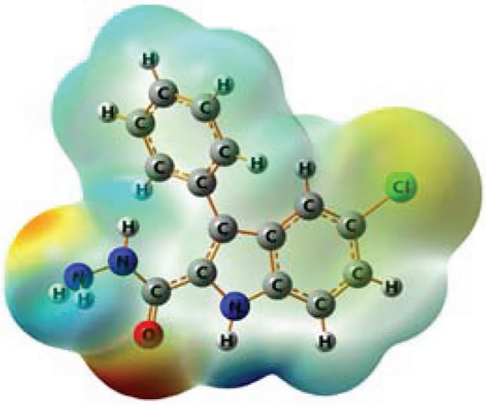

Fig. 6: Molecular electrostatic potential map

4.3.3. Multiple linear regression analysis

The spectroscopic properties $\bar{\nu}_a$, $\bar{\nu}_f$ and $\Delta\bar{\nu}$. They are correlated with the Kamlet and Catalan parameters. The solvatochromic parameters α, β, and π* are correlated from multiple regression studies to identify the different contributions of the solvents to the spectroscopic features related to Hydrogen Bond Acceptor (HBA), Hydrogen Bond Donor (HBD), and dielectric abilities. The parameters with correlation coefficients are given by the following equations [41–46].

$$\bar{\nu}_a(cm^{-1}) = 2425 + 8439 \propto -3603\beta + 973\pi^* \quad (r = 0.23) \tag{16}$$

$$\bar{\nu}_f(cm^{-1}) = 15757 + 54834 \propto -23412\beta + 2314\pi^* \quad (r = 0.50) \tag{17}$$

$$\Delta\bar{\nu}(cm^{-1}) = 15338 - 53376 \propto +22790\beta - 1455\pi^* \quad (r = 0.49) \tag{18}$$

The role of the HBD and HBA parameters cannot be disregarded. As can be seen from the relationships above, HBD (α) has a greater influence than HBA (β). The high values of α and β in comparison to π* confirm that the molecule is more sensitive to the solvent's hydrogen bonding characteristics. Eqn (15) yields correlation coefficients and the spectroscopic characteristics of the CPIC derivative, $\bar{\nu}_a$, $\bar{\nu}_f$, $and\Delta\bar{\nu}_f$, are also connected to the SA, SB, SP, and SdP solvatochromic parameters as shown in **Table 4** [47].

$$\bar{\nu}_a(cm^{-1}) = 15392 + 7067SA - 6083SB + 18589SP - 6414Sdp \ (r = 0.35) \tag{19}$$

$$\bar{\nu}_f(cm^{-1}) = 72468 + 292806SA - 21355SB + 86493SP - 29743Sdp \ (r = 0.33) \tag{20}$$

$$\Delta\bar{\nu}(cm^{-1}) = 76725 - 31007SA + 22610SB - 91574SP + 31490Sdp \ (r = 0.56) \tag{21}$$

According to the Catalan equations of CPIC, the solvent's polarizability (SP) has a higher influence than its dipolarity (SdP). On the other hand,

solvent acidity (SA) and basicity (SB) also contribute. The solvent acidity (SA) plays a vital role compared to the solvent basicity (SB).

Table 4: Kamlet and Catalan solvatochromic parameters values in different solvents

Solvents	∝	β	π^*	SA	SB	SP	SdP
DMSO	0.00	0.76	1.00	0.07	0.647	0.830	1.000
DMF	0.00	0.69	0.88	0.00	0.475	0.651	0.907
Acetonitrile	0.19	0.31	0.75	0.04	0.613	0.759	0.977
THF	0.00	0.55	0.58	0.00	0.591	0.714	0.634
EA	0.00	0.45	0.55	0.00	0.542	0.656	0.603
1,4-Dioxane	0.00	0.37	0.55	0.00	0.444	0.737	0.312
Benzene	0.00	0.1	0.59	0.00	0.124	0.793	0.270
Toluene	0.00	0.11	0.54	0.00	0.128	0.782	0.284
Cyclohexane	0.00	0.00	0.00	0.00	0.482	0.766	0.745

5. Conclusions

The ground and excited state dipole moments of the indole derivative of CPIC in various solvents were determined using the solvatochromic shift method. It is observed that the dipole moments in the excited state were larger than those in the ground state. Because the excited state is more polar than the ground state, the dipole moment in the excited state increases significantly due to the transition of π→π. The ratio of dipole moments is determined, and it is found to be minimal. The significant difference in the energy gap of the molecule, estimated by experiment and computation. The spectroscopic characteristics of the CPIC molecule are more sensitive to the solvent's polarizability and hydrogen bonding parameters of the solvent.

6. References

[1]. Xue-Hua Zhang, Yan Cui, Ryuzi Katoh, Nagatoshi Koumura and Kohjiro Hara J. Phys. Chem. C 2010, 114, 42, 18283–18290.

[2]. B. S. Mathada, N. G. Yernale, J. N. Basha, J. Badiger, an insight into the advanced synthetic recipes to access ubiquitous indole heterocycles, Tetrahedron Letters, Volume 85, 2021, 153458, https://doi.org/10.1016/j.tetlet.2021.153458.

[3]. N. G. Yernale, B. H. M. Mruthyunjayaswamy, Metal (II) complexes of ONO donor Schiff base ligand as a new class of bioactive compounds containing indole core: Synthesis and characterization, Int J Pharm Pharm Sci, Vol 8, Issue 1, 197-204 (2016).

[4]. T. Hintz, K. K. Matthews, R. Di, Biomedical Research Institute, pp.246, 2015.

[5]. C. Reichardt, T. Welton, Solvents and solvent effects in organic chemistry, John Wiley & Sons, 2011.

[6]. M. Ravi, T. Soujanya, A. Samanta, T.P. Radhakrishnan, Excited-state dipole moments of some Coumarin dyes from a solvatochromic method using the solvent polarity parameter, ENT, J. Chem. Soc., Faraday Trans. 91 (17) (1995) 2739–2742.

[7]. C. Reichardt, Solvatochromic dyes as solvent polarity indicators, Chemical reviews 94 (8) (1994) 2319–2358..

[8]. P. Suppan, Excited-state dipole moments from absorption/fluorescence solvatochromic ratios, Chem. Phys. Lett. 94 (3) (1983) 272–275, https://doi.org/10.1016/0009-2614(83)87086-9.

[9]. J.T. Edward, Molecular volumes and the Stokes-Einstein equation, J. Chem. Educ. 47 (4) (1970) 261, https://doi.org/10.1021/ed047p261

[10]. N. Kumar, M. Paramasivam, J. Kumar, A. Gusain, P.K. Hota, Tuning of optical properties of p-phenyl ethenyl-E-furans: a solvatochromism and density functional theory, Spectrochim. Acta Part A Mol. Biomol. Spectrosc. 206 (2019) 396–404, https://doi.org/10.1016/j.saa.2018.08.032.

[11]. G. G. Shivraj, B. Shivaleela and S. M. Hanagodimath, Spectroscopic analysis of NMR, IR, Raman and UV-Visible, HOMO-LUMO, ESP and Mulliken charges of coumarin derivative by density functional theory, *Journal of the Maharaja Sayajirao University of Baroda*, 55, 1 (XIV) (2021) 213-229.

[12]. G. G. Shivraj, B. Shivaleela and S. M. Hanagodimath, Comparative study of NMR, IR, Raman spectroscopy, HOMO-LUMO surfaces of benzofuran and coumarin derivative in vacuum and methanol, *Journal f the Maharaja Sayajirao University of Baroda*, 56, 2(I) (2022) 169-186.

[13]. S.M. Hanagodimath, G.C.Chikkur, G.S. Gadaginamath, Environmental effects on the energy migration coefficient, the effective energy transfer and quenching distances in an organic liquid scintillator, Chem. Phys. 148 (2) (1990) 347–357, https://doi.org/10.1016/0301-0104(90)89030-T.

[14]. S.M. Hanagodimath, G.S. Gadaginmath, G.C. Chikkur, ''Role of Brownian diffusion and interaction distance on energy transfer and quenching in an organic liquid scintillator, Int. J. Radiat. Appl. Instrument. Part A. Appl. Radiat. Isotopes 41 (9) (1990) 817–821, https://doi.org/10.1016/0883-2889(90)90058-O

[15]. S.M. Hanagodimath, G.C. Chikkur, G.S. Gadaginmath, An unique method of determining the excitation energy migration coefficient in organic liquid scintillators, Pramana – J. Phys. 37 (2) (1991) 153–161, https://doi.org/10.1007/BF02875302.

[16]. S.M. Hanagodimath, G.S. Gadaginamath, G. Chikikur, On the mechanism of excitation energy transfer involving long and short range interaction in dilute organic liquid scintillator systems, Acta Phys. Pol. A 81 (3) (1992) 361–368.

[17]. R. Melavanki, T. Muttannavar, S. Vaijayanthimala, N. Patil, L. Naik, J. Kadadevarmath, Solvent effects on the dipole moments and photo physical properties of laser dye, Indian J. Pure Appl. Phys. 56 (2018) 749–754.

[18]. V.R. Desai, S.M. Hunagund, M. Basanagouda, J.S. Kadadevarmath, J. Thipperudrappa, A.H. Sidarai, Spectroscopic studies on newly synthesized

5- (2-hydroxy-5-methoxy-phenyl)-2-phenyl-2H-pyridazin-3-one molecule, J. Mol. Liq. 225 (2017) 613–620, https://doi.org/10.1016/j.m olliq.2016.11.080.

[19]. V.R. Desai, S.M. Hunagund, M. Basanagouda, J.S. Kadadevarmath, A.H. Sidarai, Solvent effects on the electronic absorption and fluorescence spectra of HNP: estimation of ground and excited state dipole moments, J. Fluoresc. 26 (4) (2016) 1391–1400, https://doi.org/10.1007/s10895-016-1830-3.

[20]. B. Siddlingeshwar, S.M. Hanagodimath, E.M. Kirilova, G.K. Kirilov, Photophysical characteristics of three novel benzanthrone derivatives: Experimental and theoretical estimation of dipole moments, J. Quant. Spectrosc. Radiat. Transfer 112 (3) (2011) 448–456, https://doi.org/10.1016/j. jqsrt.2010.09.00.

[21]. G.B. Mathapati, P.K. Ingalgondi, O. Patil, S. Basavaraj, S.M. Hanagodimath, Estimation of ground and excited state dipole moments of newly synthesized coumarin molecule, Int. J. Scient. Res. Phys. Appl. Sci. 5 (2018) 1061–1065.

[22]. G.B. Mathapati, O. Patil, S. Basavaraj, S. Gounalli, S.M. Hanagodimat, Estimation of ground and excited state dipole moments of newly synthesized coumarin molecule by Solvatochromic shift method and Gaussian software, Int. J. sci. Res. Phys. Appl. Sci. 7 (2019) 38–43, https://doi.org/10.26438/ ijsrpas/ v7i2.3843.

[23]. Kulkarni MV, Kulkarni GM, Lin CH, Sun CM (2006) Recent advances in coumarins and 1-azacoumarins as versatile biody namic agents. Curr Med Chem 13:2795–2818.

[24]. Patil O, Ingalagondi PK, Hanagodimath SM (2021) Estimation of dipole moments of new coumarin dye by experimental and theoretical methods. Macromol Symp 400:2100015. https:// doi. org/10.1002/masy.202100015.

[25]. E. Lipert, Dipole moment and electronic structure of excited molecules, Z. Naturforsch 10 (1955) 541–546.

[26]. N. Mataga, Y. Kaifu, M. Koizumi, The solvent effect on fluorescence spectrum, change of solute-solvent interaction during the lifetime of excited solute molecule, BCSJ 28(9) (1955)690https://doi.org/10.1246/bcsj.28.690.

[27]. N.G. Bakshiev, Solvent dielectric relaxation effects, Optical Spectroscopy" 13 (1962) 507–530.

[28]. L. Bilot, A. Kawski, Zur theorie des einflusses von Lösungsmitteln auf die elektronenspektren der moleküle, Zeitschrift für Naturforschung A 17 (7) (1962) 621–627.

[29]. L.Bilot,A.Kawski,Der Einfluß des Lösungsmittels auf die Elektronenspektren lumineszierender Moleküle, Z. Naturforsch 18A (1963) 10–15.

[30]. M. Pourtabrizi, N. Shahtahmassebi, A. Kompany, S. Sharifi, Dipole moment of excited and ground state of Auramine O doped nano-droplet, Opt. Quant. Electron. 49 (9) (2017) 291, https://doi.org/10.1007/s11082-017-1124-2.

[31]. C. Reichardt, T. Welton, Solvents and solvent effects in organic chemistry, John Wiley & Sons, 2011.

[32]. M. Ravi, T. Soujanya, A. Samanta, T.P. Radhakrishnan, Excited-state dipole moments of some Coumarin dyes from a solvatochromic method using the solvent polarity parameter, ENT, J. Chem. Soc., Faraday Trans. 91 (17) (1995) 2739–2742.

[33]. C. Reichardt, Solvatochromic dyes as solvent polarity indicators, Chemical reviews 94 (8) (1994) 2319–2358..

[34]. P. Suppan, Excited-state dipole moments from absorption/fluorescence solvatochromic ratios, Chem. Phys. Lett. 94 (3) (1983) 272–275, https://doi.org/10.1016/0009-2614(83)87086-9.

[35]. J.T. Edward, Molecular volumes and the Stokes-Einstein equation, J. Chem. Educ. 47 (4) (1970) 261, https://doi.org/10.1021/ed047p261.

[36]. N. Kumar, M. Paramasivam, J. Kumar, A. Gusain, P.K. Hota, Tuning of optical properties of p-phenyl ethenyl-E-furans: a solvatochromism and density functional theory, Spectrochim. Acta Part A Mol. Biomol. Spectrosc. 206 (2019) 396–404, https://doi.org/10.1016/j.saa.2018.08.032.

[37]. V.R. Desai, S.M. Hunagund, M. Basanagouda, J.S. Kadadevarmath, J. Thipperudrappa, A.H. Sidarai, Spectroscopic studies on newly synthesized 5- (2-hydroxy-5-methoxy-phenyl)-2-phenyl-2H-pyridazin-3-one molecule, J. Mol. Liq. 225 (2017) 613–620, https://doi.org/10.1016/j.molliq.2016.11.080.

[38]. R. Kumari, A. Varghese, L. George, Synthesis, crystal structure and photophysical properties of (E)-4-(4-(2-hydroxybenzylideneamino) benzyl) oxazolidin-2-one, J. Lumin. 179 (2016) 518–526.

[39]. S.N. Patil, F.M. Sanningannavar, B.S. Navati, N.R. Patil, R.A. Kusanur, R.M. Melavanki, Spectroscopic properties and estimation of ground and excited state dipole moments of biologically active fluorescent molecule from absorption and emission spectra 4 (1) (2014) 11.

[40]. S. Sharifi, S.G. Salavatovna, A. Azarpour, F. Rakhshanizadeh, G. Zohuri, M.R. Sharifmoghadam, Optical properties of methyl orange-doped droplet and photodynamic therapy of Staphylococcus aureus, J. Fluoresc. 29 (6) (2019) 1331–1341, https://doi.org/10.1007/s10895-019-02459-0.

[41]. V.R. Desai, S.M. Hunagund, M. Basanagouda, J.S. Kadadevarmath, A.H. Sidarai, Solvent effects on the electronic absorption and fluorescence spectra of HNP: estimation of ground and excited state dipole moments, J. Fluoresc. 26 (4) (2016) 1391–1400, https://doi.org/10.1007/s10895-016-1830-3.

[42]. G.H. Pujar, M.N. Wari, B. Steffi, H. Varsha, B. Kavita, Y.C Panicker, C. Santhosh, P. Ajeetkumar, S.R. Inamdar, A combined experimental and computational investigation of solvatochromism of nonpolar laser dyes: Evaluation of ground and singlet excited-state dipole moments, J. Mol. Liq. 244 (2017) 453–463, https://doi.org/10.1016 /j.molliq.2017.08.078.

[43]. B. Siddlingeshwar, S.M. Hanagodimath, E.M. Kirilova, G.K. Kirilov, Photophysical characteristics of three novel benzanthrone derivatives: Experimental and theoretical estimation of dipole moments, J. Quant. Spectrosc. Radiat. Transfer 112 (3) (2011) 448–456, https://doi.org/10.1016/j.jqsrt.2010.09.00.

[44]. G.B. Mathapati, P.K. Ingalgondi, O. Patil, S. Basavaraj, S.M. Hanagodimath, Estimation of ground and excited state dipole moments of newly synthesized coumarin molecule, Int. J. Scient. Res. Phys. Appl. Sci. 5 (2018) 1061–1065.

[45]. G.B. Mathapati,O. Patil, S. Basavaraj, S. Gounalli, S.M.Hanagodimat, Estimation of ground and excited state dipole moments of newly synthesized coumarin molecule by Solvatochromic shift method and Gaussian software, Int.J.sci.Res.Phys Appl.Sci.7(2019) 38–43, https: //doi.org /10.26438 /ijsrpas / v7i2. 3843.

[46]. Y.G. Sidir, The solvatochromism, electronic structure, electric dipole moments and DFT calculations of benzoic acid liquid crystals, Liq. Cryst. 47 (10) (2020) 1435–1451, https://doi.org/10.1080/02678292.2020.1733685.

[47]. N. Pandey, N. Tewari, S. Pant, M.S. Mehata, Solvatochromism and estimation of ground and excited state dipole moments of 6-aminoquinoline, Spectrochim.

Conflict of Interest

The authors hereby declare no potential conflicts of interest with respect to the research, funding, authorship, and/or publication of this article